NUMERICAL IMPLEMENTATION OF AN ALGORITHM FOR DETERMINATION MULTIAXIAL FATIGUE LIMIT

Lucival Malcher, malcher@unb.br
José Carlos Balthazar, jcbalthazar@unb.br
University of Brasilia
Department of Mechanical Engineering
Brasília – DF - Brazil

Abstract. *The estimation of fatigue strength or fatigue life of a component under combined loading is fundamental to correct design and safe operational life of many structural components. The fatigue process under complexes states of stresses generated in these situations is known as Multiaxial Fatigue. In the present work the algorithm for determination multiaxial fatigue limit is developed and implemented, based in the ellipsoid simplified circumscribed model, proposed for Balthazar e Malcher (2006). A theoretical revision of the model as well as a quantitavive analysis is made. To the end, a comparison of the results presented with the other available models in literature became.*

Keywords*: numerical implementation, multiaxial fatigue limit, out-of-phase loading, stress invariant, ellipsoid simplified model*

1. INTRODUCTION

Most of structural mechanical components are frequently subjected to variable loading, which can lead to sudden fatigue failure. Crank drive shafts, pressure vessels, blade/rotor junctions, bolted junctions and many aeronautical components are usually operating under combined loads which can still be out of phase and in different frequencies generating complexes biaxial or triaxial states of stresses. The fatigue process under such states of stresses is known as Multiaxial Fatigue whose consideration is of fundamental importance for assessment of life and operational reliability of structural components. Therefore, efficient and accurate methodologies for the evaluation of fatigue endurance limit under multiaxial stress states are required for use in engineering design applications.

Although many important developments have been made over more than hundred of research on the subject, many designers still resort to large factors of safety to guard structural components against fatigue failures. The first attempts to investigate problems of multiaxial fatigue go back to the end of 19th century when Lanza (1886) published results of tests concerning combined bending/torsion loading. In the early decades of the 20th century, investigators like Mason (1917), Haigh (1923), Nishiara and Kawamoto (1941) and Gough et al (1951) presented empirical relations obtained from experimental data. The initial theories proposed to predict fatigue failure under combined loading were basically an extension of the failure theories for static multiaxial state of stress to multiaxial states of cyclic stresses. The aim of these theories was to produce an uniaxial stress amplitude equivalent to a given multiaxial cyclic stress states and then use it to predict fatigue life from S-N curves, obtained from conventional fatigue tests. The Maximum Shearing Stress Theory of Fatigue Failure and the Distortion Energy Multiaxial Theory of Fatigue Failure (1981) were basically extensions of the Tresca and von Mises theories, respectively. The stress amplitudes were substitutes for the static principal stresses and the reversed fatigue strength or fatigue limit replaced the yield stress. The experimental evidence showed these methods were very conservative. The models for multiaxial fatigue analysis are generally divided into three groups: the stress-based models, strain-based models and energy models.

For multiaxial high cycle fatigue – HCF analysis, a number of criteria, derived from different approaches to the problem, have been reviewed in the literature (1981, 2004), the equivalent stress, the critical plane, the average stress and the stress invariant methods, are the most known approaches for the problem.

In the present work the algorithm for determination multiaxial fatigue limit is developed and implemented, based in the ellipsoid simplified circumscribed model, proposed for Malcher & Balthazar (2006).

2. MULTIAXIAL HIGH CYCLE FATIGUE MODELS

Many mechanical components, like the hydraulic turbines used in the power generating industry, are designed to endure a very large number of cycles without failure. Their size and operational conditions make impractical frequent stoppages for inspection and maintenance and, consequently, the use of Fracture Mechanics approaches for failure control. In the high cycle fatigue regime, most of total life is spent to initiate a crack of detectable size by non-destructive inspection. Thus, in these cases, it would be preferable to design against HCF, considering a criterion for crack initiation in order to keep structures under dynamic loading operating safely. To achieve this objective, a domain of safety, limited by a threshold below which cracks will not initiate, must be calculated.

The degradation of the state of the material under HCF occurs at stress levels well below the yield limit. The fatigue damage is related to cyclic plastic deformations at the grain level, followed by the formation of persistent slip bands from which microcracks will be nucleated, even in materials under elastic regime at macroscopic level. Therefore, shear

stresses must be considered as one of the driving forces of the fatigue process. The normal stresses, which act upon the initiating crack, will also affect the fatigue resistance.

2.1. The Stress Invariant Methods

The invariant stress approach is based on the invariants of the stress tensor and/or its deviator tensor. The basic idea is to directly relate the fatigue strength with the second invariant of the stress deviator and first invariant of the stress (3 times the hydrostatic stress). The initiation of a fatigue crack under cyclic loading would be predicted when the left side of the equation below gets bigger than the right side:

$$\sqrt{J_{2,a}} + k(N).\sigma_H \leq \lambda(N) \tag{1}$$

where, $\sqrt{J_{2,a}}$ is the equivalent shear stress amplitude, σ_H is the hydrostatic stress and $k(N)$ and $\lambda(N)$ are parameters to be experimentally determined.

Some models which use only the first invariant of the stress tensor and the second invariant the deviator tensor can be regarded as a combination of the equivalent stress approach, as it uses a shear stress equivalent to the multiaxial applied stresses, and the critical plane approach, as it searches for the maximum values of their parameters in a plan with the greatest intersection with the path of the deviatory stress tensor. The models of Sines (1955), Crossland (1956) and Kakuno-Kawada (1979) can be also be classified in this category are good representatives of this kind of approach.

The criteria of Sines (1955) and Crossland (1956) can be written in a general form as:

$$g(\tau) + f(\sigma) \leq \lambda \tag{2}$$

where, f and g are functions of the shear stress τ and the normal stress σ, respectively. The Sines criterion is mathematically expressed as:

$$\sqrt{J_{2,a}} + k\sigma_{H,mean} \leq \lambda \tag{3}$$

where, $\sqrt{J_{2,a}}$ is the equivalent shear stress amplitude and $\sigma_{H,mean}$ is the mean hydrostatic stress. The parameters k and λ are material constants, which can be obtained from two simple fatigue tests: the repeated bending limit f0 (σa = σm = f0) and the fully reversed torsion limit t-1 (τa = t-1 , τm = 0).

$$k = \left(\frac{3t_{-1}}{f_0}\right) - \sqrt{3} \quad ; \quad \lambda = t_{-1} \tag{4}$$

Instead of the mean hydrostatic stress, the Crossland criterion considers the influence of the maximum hydrostatic stress, $\sigma_{H,\max}$:

$$\sqrt{J_{2,a}} + k\sigma_{H,\max} \leq \lambda \tag{5}$$

The parameters k and λ can be also obtained from two simple fatigue tests: the fully reversed bending limit f-1 (σa = f-1 , σm = 0) and the fully reversed torsion limit t-1 (τa = t-1 , τm = 0).

$$k = \left(\frac{3t_{-1}}{f_{-1}}\right) - \sqrt{3} \quad ; \quad \lambda = t_{-1} \tag{6}$$

Kakuno and Kawada suggested that the contribution of the invariant of the stress deviator and the hydrostatic stress should be different:

$$\sqrt{J_{2,a}} + k.\sigma_{H,a} + \lambda.\sigma_{H,m} \leq \mu \tag{7}$$

where, the parameters k, λ e μ should be determined from three uniaxial fatigue limits: f_0, t_{-1} e f_{-1} (repeated bending, fully reversed torsion, fully reversed bending). Thus,

$$k = \left(\frac{3t_{-1}}{f_{-1}}\right) - \sqrt{3}\ ;\ \lambda = \left(\frac{3t_{-1}}{f_0}\right) - \sqrt{3}\ ;\ \mu = t_{-1} \tag{8}$$

For these criteria, failure will occur when the left side of the equation gets greater than the right side.

2.2. The Maximum Hydrostatic Stress

The hydrostatic stress can be determined in function of hydrostatic tensor $\underline{\underline{\sigma}}$. It is equivalent the first invariant of the stress tensor.

$$\sigma_H = \frac{1}{3}\left(tr\underline{\underline{\sigma}}\right) = \frac{1}{3}(\sigma_{xx} + \sigma_{yy} + \sigma_{zz}) \tag{9}$$

On the cyclic loading, the hydrosttic stress is a function of the time $\sigma_H(t)$ and the mean hydrostatic stress and the hydrostatic stress amplitude can be determine through the relationship between the greater and minor trace of the Cauchy tensor.

$$\sigma_{Ha} = \frac{1}{2}\left(\max\frac{tr\left(\underline{\underline{\sigma}}(t)\right)}{3} - \min\frac{tr\left(\underline{\underline{\sigma}}(t)\right)}{3}\right);\ \sigma_{Hm} = \frac{1}{2}\left(\max\frac{tr\left(\underline{\underline{\sigma}}(t)\right)}{3} + \min\frac{tr\left(\underline{\underline{\sigma}}(t)\right)}{3}\right) \tag{10}$$

The maximum hydrostatic stress can be determined for:

$$\sigma_{H\max} = \sigma_{Hm} + \sigma_{Ha} \tag{11}$$

2.3. The Equivalent Shear Stress Amplitude

The basic difference in the application of the models based on the invariants of the stress tensors, as the models of Sines (1955), Crossland (1956) and Kakuno-Kawada (1979), is the value, mean or maximum, of the hydrostatic stress σ_H used and the way to calculate the parameter $\sqrt{J_{2,a}}$. The definition of hydrostatic stress is well established and no greater difficulty to calculate it exists. The definition of the equivalent shear stress amplitude $\sqrt{J_{2,a}}$ is more complicated.

When the applied cyclic loading is uniaxial or in-phase multiaxial, the equivalent shear stress amplitude $\sqrt{J_{2,a}}$ can be determined directly taking the square root of the second invariant of the deviatory tensor:

$$\sqrt{J_{2,a}} = \sqrt{\frac{1}{6}\left\{\left(\sigma_{xx,a} - \sigma_{yy,a}\right)^2 + \left(\sigma_{yy,a} - \sigma_{zz,a}\right)^2 + \left(\sigma_{zz,a} - \sigma_{xx,a}\right)^2 + 6.\left(\tau_{xy,a}{}^2 + \tau_{yz,a}{}^2 + \tau_{xz,a}{}^2\right)\right\}} \tag{12}$$

However, when the applied cyclic loading is out-of-phase multiaxial, the determination of $\sqrt{J_{2,a}}$ is not so simple, requiring complex mathematical calculations. The vector representing the equivalent shear stress amplitude has its direction and magnitude varying along the cycle. Fig. 1(a) shows how the shear stress amplitude varies along the cycle on a proportional and non-proportional loading;

On the point under study, a generic plane Δ can be defined by its unit normal vector n, described by the spherical angles φ and θ, Fig. 1(b). The stress vector Sn acting on a such plane can be decomposed in its normal vector N and the shear stress vector C.

During the load cycle, the tip of the vector Sn describes a closed space curve ψ whose projection on plane Δ is the path of the shear stress vector C on that plane, ψ', Figure 1(c). The shear stress amplitude Ca depends on the orientation of plane Δ, thus Ca = f(φ,θ). To determine the maximum shear stress amplitude Ca,max is necessary to search the maximum of Ca = f(φ,θ) over the angles φ and θ. The critical plane approach requires to find the normal stress and shear stress amplitudes and mean values on each plane Δ passing by the point of interest and then searching

the critical plane. For stress invariant approaches, the amplitude of the equivalent shear stress $\sqrt{J_{2,a}}$ remains the same for any orientation of the plane Δ.

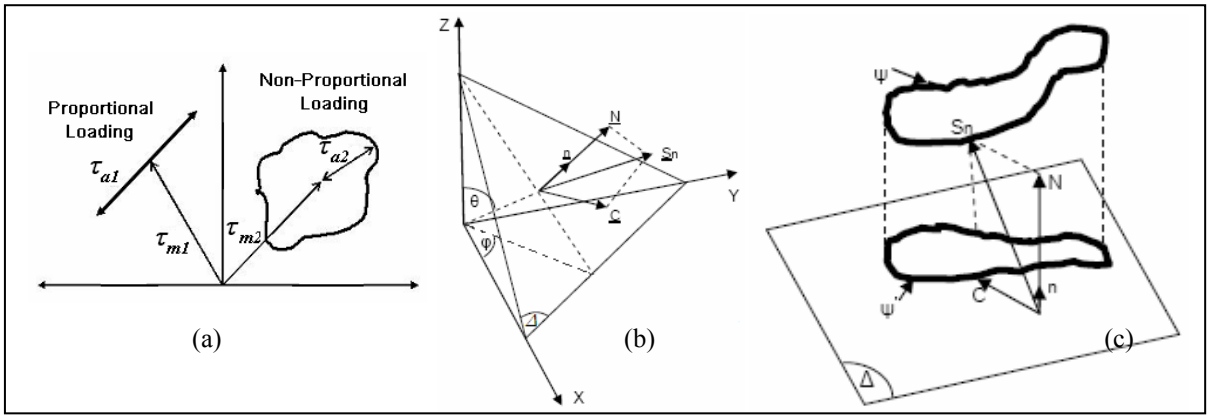

Figure 1 – (a) Behaviour of the shear stress amplitude under proportional and non-proportional loading. (b) Stress vector Sn , normal stress N and shear stress vector C acting on generic plane Δ. (c) Load paths ψ described by the stress vector Sn and ψ' described by the shear stress vector C on a generic plane Δ.

Different methods to calculate the equivalent shear stress amplitude were proposed by Dang Van et al (1988), Deperrois (1991), Duprat et al (1997), Bin Li et al (2000), Mamiya and Araújo (2002) and Balthazar and Malcher (2004) which will be described next.

2.3.1. The Minimum Circumscribed Hypersphere Method

Dang Van and Papadopoulos (1988) proposed the shear stress amplitude to be the radius C_a of the minimum hypersphere circumscribing the loading path ψ'. The mean value of the shear stress is the length of the vector w that points from the origin O to the center of the minimum circumscribed hypersphere, Cm , Figure 2. To facilitate the calculation of $\sqrt{J_{2a}}$, the following transformation is used:

$$S_1 = \frac{\sqrt{3}}{2}\bar{S}_{xx}\,,\; S_2 = \frac{1}{2}\left(\bar{S}_{yy} - \bar{S}_{zz}\right),\; S_3 = \bar{S}_{xy}\,,\; S_4 = \bar{S}_{xz}\,,\; S_5 = \bar{S}_{yz} \tag{13}$$

With the above rules the general six components of the deviatory stress may be transformed into a five component stress vector, allowing the stress deviator to be fully described by fewer components in the transformed space.

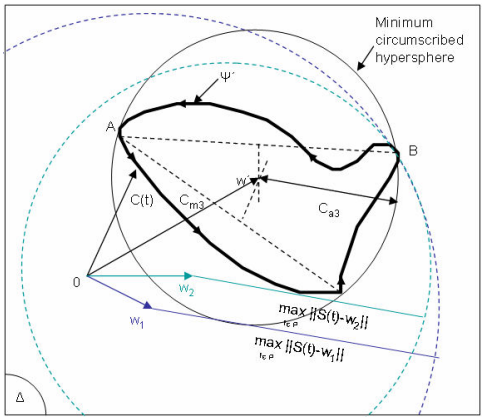

Figure 2: The Minimum Circumscribed Hypersphere Model.

The center w' and the radius R are determined by the following equations:

$$w': \min_{w}\left(\max\|S(t)-w\|\right); R=\max_{t}\left\|S(t)-w'\right\| \tag{14}$$

2.3.2. The Minimum Circumscribed Ellipsoid Method

An approach to determine the equivalent shear stress amplitude taking in account the effect of the phase angle was proposed by Bin Li et al (2002). Instead of circumscribing the loading path ψ' by a minimum hypersphere, Bin Li and his colleagues suggest to consider the minimum circumscribed ellipsoid to calculate $\sqrt{J_{2a}}$. The value of the equivalent shear stress would be then:

$$\sqrt{J_{2a}}=\sqrt{R_a^2+R_b^2} \tag{15}$$

where, R_a and R_b are the two semi-axis of an ellipse circumscribing the loading path ψ'. This method requires a two step procedure for the determination of $\sqrt{J_{2a}}$, figure 3. Firstly, a minimum circumscribed circle of radius R_a, equal to the ellipse great semi-axis, is established according the minimum circumscribed hypersphere method, described above. The small semi-axis R_b is the determined from the minimum ellipse contained in the circle and also containing the loading path ψ'.

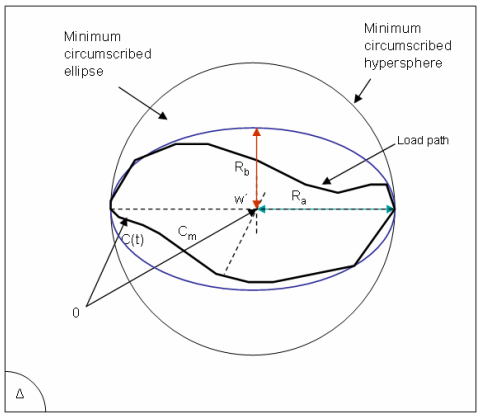

Figure 3: The minimum circumscribed ellipsoid method.

This model takes in account the effect of non-proportional loads on fatigue life and presents good results for multiaxial fatigue strength, when compared to the other methods, but it also presents the same difficulties of the Dang Van and Papadopoulos method to determine the center of the minimum circumscribed circle, which is also the center of the minimum circumscribed ellipse.

2.3.3. The Minimum Prismatic Envelope Method

Mamiya e Araújo (2002) proposed, instead of hypersphere or ellipsoid, the construction of a prismatic envelope containing the loading path projected on the deviatory plane, Figure 4. The equivalent shear stress amplitude could then be calculated by the following equations:

$$\sqrt{J_{2a}}=\left(\sum_{i=1}^{5}a_i^2\right)^{\frac{1}{2}};\ a_i=\max_{i}\left|x_i(t)\right| \tag{16}$$

where, a_i are the amplitudes of the components $x_i(t)$ of the microscopic deviatory stresses.

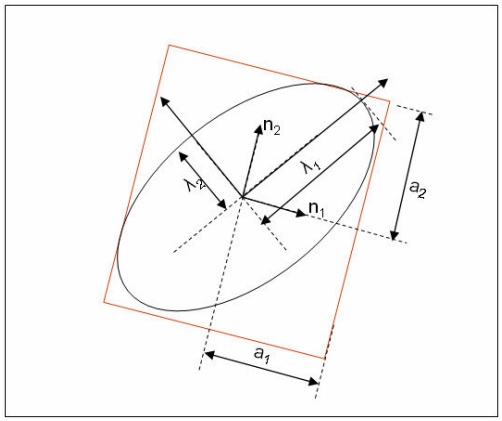

Figure 4: Ellipsoid in the R^m space and circumscribed rectangular prism arbitrarily oriented.

2.3.4. The Minimum Simplified Circumscribed Ellipsoid Method

Duprat et al (1997) proposed a method, which could consider the phase angle in tension-bending and torsion stress loading. The model is derived from Crossland criteria, using the projection of the stress tensor path on the deviatory plane. This projection is an ellipse of long axis D and short axis d, Figure 5. While Crossland original formula uses only D in the calculation of $\sqrt{J_{2a}}$, Duprat et al replaces D by the half-perimeter of the ellipse, $\frac{p_e}{2}$, to take in account the phase difference, characterized by D and d.

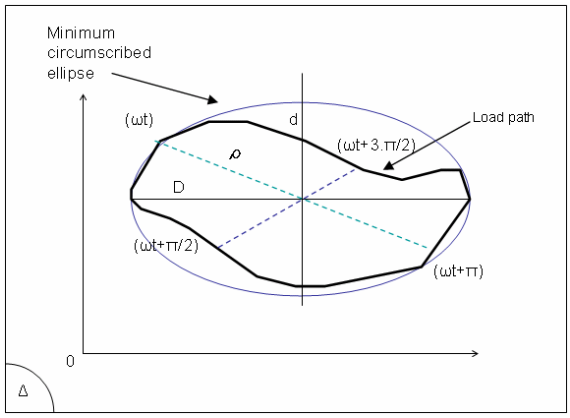

Figure 5: Projection of the tensor path on the deviatory plane.

The values of D and d are given by:

$$D = \max(t)\rho(\omega t); d = \min(t)\rho(\omega t) \tag{17}$$

with the parameter $\rho(\omega t)$ being:

$$\rho(\omega t) = tr\left[\left(\underline{\underline{S}}(t) - \underline{\underline{S}}(t+\pi)\right)\left(\underline{\underline{S}}(t) - \underline{\underline{S}}(t+\pi)\right)\right]^{\frac{1}{2}} \tag{18}$$

where, $\underline{\underline{S}}(t)$ is the deviatory stress tensor .

The value of the equivalent shear stress amplitude $\sqrt{J_{2a}}$ is function of the ellipse half-perimeter $p_e/2$:

$$\sqrt{J_{2a}} = \frac{1}{2}\cdot\frac{p_e/2}{\sqrt{2}}; \frac{p_e}{2} \approx \frac{\pi}{2}\cdot\frac{D+d}{2}\cdot\left[1+\frac{1}{4}\lambda^2+\frac{1}{64}\lambda^4+\frac{1}{256}\lambda^6\right]; \lambda = \frac{D-d}{D+d} \tag{19}$$

Malcher & Balthazar (2006) showed the application of this method results in increased scatter for larger phase angles between the applied loads. They showed that a reduction on such scattering could be obtained combining the proposal of Duprat et al (1997) with the minimum circumscribed ellipsoid method proposed by Bin Li et al (2000). The equivalent shear stress amplitude could be calculated as proposed by Bin Li:

$$\sqrt{J_{2a}} = \sqrt{R_a^2 + R_b^2} \tag{20}$$

but using the values of the ellipse semi-axis from the model of Duprat. Thus:

$$R_a = \frac{D}{2} = \frac{\max(t)\rho(\omega t)}{2}; R_b = \frac{d}{2} = \frac{\min(t)\rho(\omega t)}{2} \tag{21}$$

The equivalent shear stress amplitude would be then given by:

$$\sqrt{J_{2a}} = \frac{1}{2}\frac{\sqrt{[\max(t)\rho(\omega t)]^2 + [\min(t)\rho(\omega t)]^2}}{\sqrt{2}} \tag{22}$$

The main advantage of this modification is the simplicity added to the equivalent shear stress amplitude calculations, as it is easier to determine the ellipse semi-axis D/2 and d/2 as proposed by Duprat than the complex calculations required to obtain the center of the minimum circumscribed hyperesphere or ellipsoid, necessary for the methods of Dang Van, Papadopoulos and Bin Li. Thus, the criterion for multiaxial fatigue can be expressed as:

3. ALGORITHM FOR IMPLEMENTATION THE MALCHER & BALTHAZAR METHOD

The figure 6 shows step by step to implement at algorithm developed for Malcher and Balthazar model (2006). It´s necessary informant the path loading and the material propriety. After, the Cauchy Tensor and Deviator Tensor are defined. The maximum and minimum trace of Cauchy Tensor and the parameter $\rho(\omega t)$ of the Deviator Tensor are searched with increment of the one by one degree of the phase angle. The maximum hydrostatic stress and the equivalent shear stress amplitude can be determined. The end, the index of error and the ratio of stress are calculated.

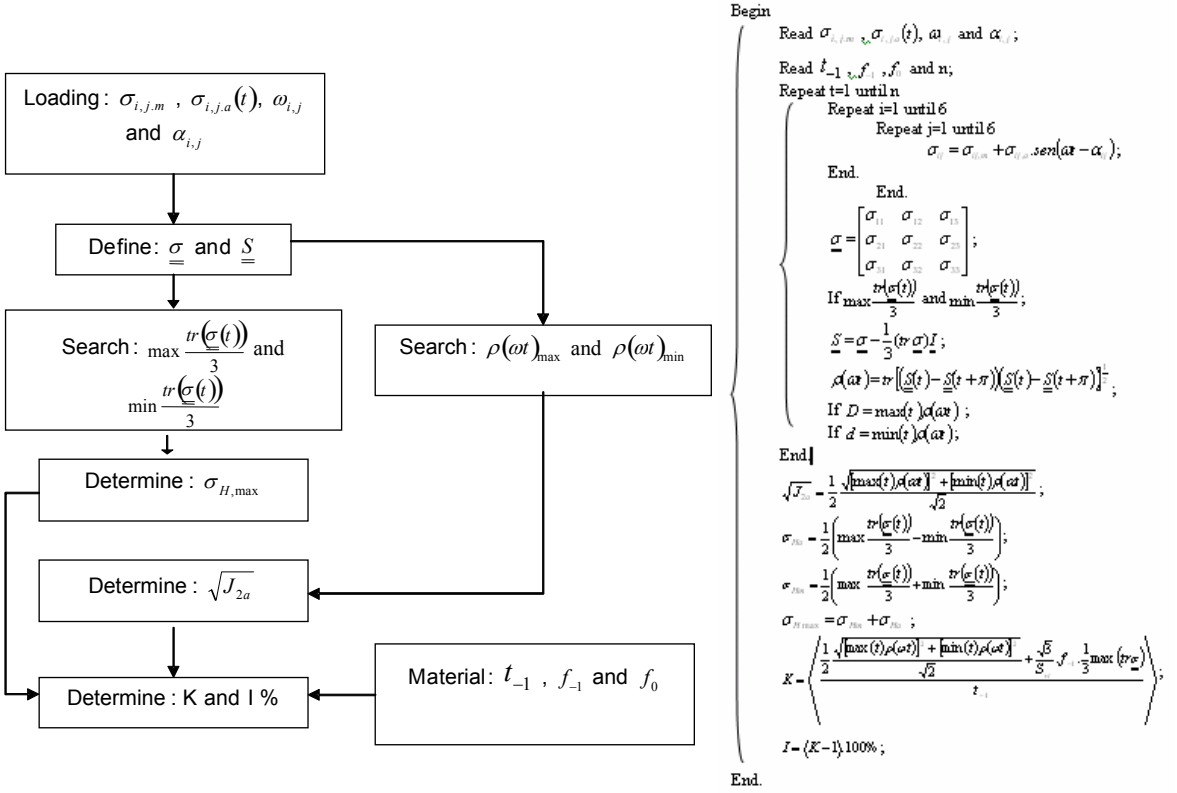

Figure 6: Algorithm for Malcher and Balthazar Model.

4. RESULTS

Experimental data obtained in the literature was used to test the algorithm and the results were comparated with Papadopoulos model. It was used 32 results from biaxial constant amplitude loading, from in-phase and out-of-phase tests conducted by Zener et al, 1985 on 34Cr4 steel (group: 100 – test: traction+torsion); by Froustey and Lasserre, 1988 on 30NCD16 (group: 200 – test: beding+torsion) and by Nishihara and Kawamoto, 1945 on Hard steel (group: 300 – test: beding+torsion) as reported by Weber(1999) and Papadopoulos(1993).

Defining the equivalent stress σ_{eq} to the fully reversed torsional fatigue limit t_{-1} ratio as $K = \sigma_{eq} / t_{-1}$, it is possible to assess the quality the predictions made by each model. If K=1 the model predict perfectly the multiaxial fatigue behaviour. If K is higher than 1, the predictions are conservative. An index of error I can be also established as $I = (K-1)\times 100$. Tables 1 to 3 and figure 3 show the data applied to test the Malcher & Balthazar and Papadopoulos models.

Table 1 – Experimental data for 34Cr4 steel

Group	Test	Steel	f-1	f0	t-1	N	σ11m	σ11a	σ12m	σ12a	α12
100	101	34Cr4	410	640	256	1500000	0	314	0	157	0
100	102	34Cr4	410	640	256	1500000	0	315	0	158	60
100	103	34Cr4	410	640	256	1500000	0	316	0	158	90
100	104	34Cr4	410	640	256	1500000	0	315	0	158	120
100	105	34Cr4	410	640	256	1500000	0	224	0	224	90
100	106	34Cr4	410	640	256	1500000	0	380	0	95	90
100	107	34Cr4	410	640	256	1500000	0	316	158	158	0
100	108	34Cr4	410	640	256	1500000	0	314	157	157	60
100	109	34Cr4	410	640	256	1500000	0	315	158	158	90
100	110	34Cr4	410	640	256	1500000	279	279	0	140	0
100	111	34Cr4	410	640	256	1500000	284	284	0	142	90
100	112	34Cr4	410	640	256	1500000	212	212	0	212	90

Table 2 – Experimental data for 30NCD16 steel

Group	Test	Steel	f-1	f0	t-1	N	σ11m	σ11a	σ12m	σ12a	α12
200	201	30NCD16	695	1040	415	1000000	0	485	0	280	0
200	202	30NCD16	695	1040	415	1000000	0	480	0	277	90
200	203	30NCD16	695	1040	415	1000000	300	480	0	277	0
200	204	30NCD16	695	1040	415	1000000	300	480	0	277	45
200	205	30NCD16	695	1040	415	1000000	300	470	0	271	60
200	206	30NCD16	695	1040	415	1000000	300	473	0	273	90
200	207	30NCD16	695	1040	415	1000000	300	590	0	148	0
200	208	30NCD16	695	1040	415	1000000	300	565	0	141	45
200	209	30NCD16	695	1040	415	1000000	300	540	0	135	90
200	210	30NCD16	695	1040	415	1000000	300	211	0	365	0

Table 3 – Experimental data for Hard steel

Group	Test	Steel	f-1	f0	t-1	N	σ11m	σ11a	σ12m	σ12a	α12
300	301	Hard steel	314	512	196		0	138	0	167	0
300	302	Hard steel	314	512	196		0	245	0	123	0
300	303	Hard steel	314	512	196		0	299	0	63	0
300	304	Hard steel	314	512	196		0	140	0	170	30
300	305	Hard steel	314	512	196		0	146	0	176	60
300	306	Hard steel	314	512	196		0	150	0	182	90
300	307	Hard steel	314	512	196		0	250	0	125	30
300	308	Hard steel	314	512	196		0	252	0	126	60
300	309	Hard steel	314	512	196		0	258	0	129	90
300	310	Hard steel	314	512	196		0	305	0	64	90

Tables 4 to 6 show the values of $\sigma_{H,\max}$, $\sqrt{J_{2a}}$, σ_{eq}, I and K for Malcher & Balthazar and Papadopoulos models. Notwithstanding the results given by both models were similar. The present algorithm proposal represents a simplified way to determine the equivalent shear stress amplitude, eliminating the need the complex calculations required by the other methods, without losing quality in the results.

It can be observed that the maximum error lies around 6% on 34Cr4 steel, 14% on 30NCD16 steel and 6% on Hard steel when the phase angle between the applied loads is 90º.

Table 4 – Results given by Malcher & Balthazar and Papadopoulos for 34Cr4 steel

Group	Test	Steel	α12	Malcher&Balthazar					Papadopoulos				
				σHmax	√J2a	σeq	K	I	σHmax	√J2a	σeq	K	I
100	101	34Cr4	0	104,7	239,8	254,6	0,99	-0,6	104,7	239,8	254,6	0,99	-0,6
100	102	34Cr4	60	105,0	240,9	255,7	1,00	-0,1	105,0	240,9	255,7	1,00	-0,1
100	103	34Cr4	90	105,3	241,4	256,2	1,00	0,1	105,3	241,4	256,2	1,00	0,1
100	104	34Cr4	120	105,0	240,9	255,7	1,00	-0,1	105,0	240,9	255,7	1,00	-0,1
100	105	34Cr4	90	74,7	258,7	269,2	1,05	5,2	74,7	258,6	269,2	1,05	5,2
100	106	34Cr4	90	126,7	239,1	257,0	1,00	0,4	126,7	239,1	257,0	1,00	0,4
100	107	34Cr4	0	105,3	241,4	256,2	1,00	0,1	105,3	241,4	256,2	1,00	0,1
100	108	34Cr4	60	104,7	239,8	254,6	0,99	-0,6	104,7	239,8	254,6	0,99	-0,6
100	109	34Cr4	90	105,0	240,9	255,7	1,00	-0,1	105,0	240,9	255,7	1,00	-0,1
100	110	34Cr4	0	186,0	213,4	239,7	0,94	-6,4	186,0	213,4	239,7	1,06	6,4
100	111	34Cr4	90	189,3	216,9	243,6	0,95	-4,8	189,3	216,9	243,6	0,95	-4,8
100	112	34Cr4	90	141,3	244,8	264,7	1,03	3,4	141,3	244,8	264,7	1,03	3,4

Table 5 – Results given by Malcher & Balthazar and Papadopoulos for 30NCD16 steel

Group	Test	Steel	α12	Malcher&Balthazar					Papadopoulos				
				σHmax	√J2a	σeq	K	I	σHmax	√J2a	σeq	K	I
200	201	30NCD16	0		396,0	405,6	0,98	-2,3	161,7	396,0	417,3	1,02	1,8
200	202	30NCD16	90	160,0	391,8	401,3	0,97	-3,3	160,0	391,8	412,9	1,01	0,7
200	203	30NCD16	0		391,8	407,3	0,98	-1,9	260,0	391,8	426,0	1,04	3,9
200	204	30NCD16	45		391,8	407,3	0,98	-1,9	260,0	391,8	426,0	1,04	3,9
200	205	30NCD16	60	256,7	383,5	398,7	0,96	-3,9	256,7	382,8	416,0	1,02	1,6
200	206	30NCD16	90	257,7	386,1	401,4	0,97	-3,3	257,7	386,1	420,0	1,03	2,5
200	207	30NCD16	0		371,4	389,0	0,94	-6,3	296,7	371,4	410,4	1,00	0,1
200	208	30NCD16	45	288,3	355,4	372,5	0,90	-10,3	288,3	355,4	393,3	0,96	-4,1
200	209	30NCD16	90	280,0	339,7	356,4	0,86	-14,1	280,0	339,7	376,6	0,92	-8,1
200	210	30NCD16	0		384,8	394,9	0,95	-4,8	170,3	384,8	407,2	0,99	-0,7

Table 6 – Results given by Malcher & Balthazar and Papadopoulos for Hard steel

Group	Test	Steel	α12	Malcher&Balthazar					Papadopoulos				
				σHmax	√J2a	σeq	K	I	σHmax	√J2a	σeq	K	I
300	301	Hard steel	0	46,0	185,0	191,5	0,98	-2,3	46,0	185,1	191,7	0,98	-2,3
300	302	Hard steel	0	81,7	187,5	198,9	1,01	1,5	81,8	187,4	199,0	1,02	1,5
300	303	Hard steel	0	99,7	183,8	197,8	1,01	0,9	99,7	183,8	198,0	1,01	0,9
300	304	Hard steel	30	46,7	188,2	194,8	0,99	-0,6	46,8	188,2	194,9	0,99	-0,6
300	305	Hard steel	60	48,7	195,1	202,0	1,03	3,1	48,6	195,3	202,3	1,03	3,1
300	306	Hard steel	90	50,0	201,6	208,6	1,06	6,4	50,1	201,3	208,5	1,06	6,3
300	307	Hard steel	30	83,3	190,9	202,7	1,03	3,4	83,2	190,7	202,6	1,03	3,3
300	308	Hard steel	60	84,0	192,5	204,3	1,04	4,2	84,1	192,8	204,8	1,04	4,4
300	309	Hard steel	90	86,0	197,1	209,1	1,07	6,7	86,0	197,1	209,4	1,07	6,7
300	310	Hard steel	90	101,7	187,4	201,7	1,03	2,9	101,5	187,1	201,6	1,03	2,7

5. CONCLUSIONS

The present paper showed that the Malcher and Balthazar presents a simplified algorithm to determine the equivalent shear stress amplitude and the fatigue limit, eliminating the need the complex calculations required by the

other methods without losing quality in the results. The tables 4, 5 and 6 showed comparative results for Malcher & Balthazar model and Papadopoulos models. Papadopoulos tries to determinate this parameter through the minimum circle circumscribing the path of the deviatory stress tensor. The models present similar results with the difference lying on the method to calculate the equivalent shear stress amplitude $\sqrt{J_{2a}}$.

6. REFERENCES

BALTHAZAR, J.C., MALCHER, L., A review on the main approaches for determination of the multiaxial high fatigue strength. Solid Mechanics in Brazil 2007. Brazilian Society of Mechanical Sciences and Engineering, 2007, v. 1, p. 63-80;

BIN LI, SANTOS, J.L.T., FREITAS, M., A Unified Numerical Approach for Multiaxial Fatigue Limit Evaluation, Mech. Struct. & Mach., Vol. 28, 1, 2000, p.p. 85-103;

CROSSLAND, B. Effect of large hydrostatic pressures on the torsional fatigue strength of an alloy steel, in: Proc. Int. Conf. on Fatigue of Metals, IMechE, London, 1956, pp. 138–149;

DANG VAN, K., Sur la Résistance à la fatigue des Métaux. Sciencies et Technique de L' armement, 1973, 47, 429-453 ;

DEPERROIS, A., Sur le Calcul de Limites D'Endurance des Aciers, These de Doctorat, Ecole Polytechnique, 1991, Paris ;

DUBAR, L., Fatigue multiaxiale des aciers. Passage de I'endurance à I'endurance limiteé. Prise en compte des accidents géométriques.Thèse de I'ENSAM, Talence, Juin 1992, 165 p ;

DUPRAT, D., BOUDET, R., DAVY, A., A Simple Model to Predict Fatigue Strength with Out-of Phase Tension-Bending and Torsion Stress Condition, Proc. 9th Int. Conf Fracture, Sidney, Australia, 1997, p.p. 1379-1386;

KAKUNO H., KAWADA Y., A New Criterion of Fatigue Strength of a Round Bar Subjected to Combined Static and Repeated bending and Torsion, Fatigue Engng Mat Struct, 1979, Vol. 2, pp. 229-236;

LEMPP, W., Festigkeitsverhalten von stählen bei mehrachsiger dauerschwingbeanspruchung durch normalspannungen mit überlagerten phasengleichen und phasenverschobenen schubspannungen. Diss. TU Stuttgard, 1977;

MALCHER, L. (2006). Um Modelo para Determinação da Resistência à Fadiga Multiaxial para Carregamentos de Flexão e Torção Combinados, Fora de Fase e com Amplitude Constante. Com Base no Critério do Invariante do Tensor. Dissertação de Mestrado, Publicação ENM.DM-105A/06, Departamento de Engenharia Mecânica, Universidade de Brasília,DF, 88 p;

MALCHER, L., BALTHAZAR, J.C., An Analysis of the Ellipsoid Simplified Model for Determination of the Fatigue Strength in Biaxial/Triaxial Loading and Out-of-Phase, Proc.16ºPOSMEC - 16º Simpósio de Pós-Graduação em Engenharia Mecânica, Uberlandia, Brazil, 2006;

MAMIYA, E. N., ARAUJO, J. A., Fatigue Limit Under Multiaxial Loadings: On The Definition of The Equivalent Shear Stress. Mechanics Research Communications, 2002, V29, pp 141-151;

NISHIHARA, T., KAWAMOTO, M., The Strength of metals under combined alternating bending and torsion with phase difference. Memoirs of College of Engineering, Kyoto Imperial University, 1945, Vol. 11, Nº 5, pp. 85-112;

PAPADOPOULOS, I.V. and DANG VAN, K., Sur la Nucleation des Fissures en Fatigue Polycyclique sous Chargement Multiaxial, Arch. Mech., Vol. 40, 1988, p.p. 759-774

PAPADOPOULOS, I. V., A review of multiaxial fatigue limit criteria . ECJRC, SMU, Ispra, (Va), 1992 ;

SIMBÜGER, A., Festigkeitsverhalten zäher werkstoffe bei einer mehrachsigen phasenverschobenen schwingbeanspruchug mit körperfesten und veränderlichen hauptspannungrichtungen. L.B.F., Darmstadt, Bericht, 1975, Nr.FB-121,247 p;

SINES, G., Failure of materials under combined repeated stresses with superimposed static stresses, NACA Technical Note 3495, Washington, USA, 1955;

WEBER, B., Fatigue multiaxiale des structures industrielles sous chargement quelconque. Thèse de Ingénieur de I'Institut National des Sciences Appliquées de Lyon, 1999, 247 p ;

7. RESPONSIBILITY NOTICE

The authors are the only responsible for the printed material included in this paper.